Supplementary Information

Catalytic Atroposelective Synthesis of Axially Chiral Benzonitriles via Chirality Control during Bond Dissociatoin and CN Group Formation

Ya Lv,[1] Guoyong Luo,[2] Qian Liu,[1] Zhichao Jin,[1]* Xinglong Zhang[4]* and Yonggui Robin Chi[1,3]*

[1]State Key Laboratory Breeding Base of Green Pesticide and Agricultural Bioengineering, Key Laboratory of Green Pesticide and Agricultural Bioengineering, Ministry of Education, Guizhou University, Huaxi District, Guiyang 550025, China.

[2]School of Pharmacy, Guizhou University of Traditional Chinese Medicine, Huaxi District, Guiyang 550025, China.

[3]Division of Chemistry & Biological Chemistry, School of Physical & Mathematical Sciences, Nanyang Technological University, Singapore 637371, Singapore.

[4]Institute of High Performance Computing, A*STAR (Agency for Science, Technology and Research), Singapore 138632, Singapore.

*Corresponding authors e-mails:

zcjin@gzu.edu.cn

Zhang_Xinglong@ihpc.a-star.edu.sg

robinchi@ntu.edu.sg.

Density functional theory (DFT) calculations

Computational methods

Density functional theory (DFT) calculations were performed with *Gaussian 16* rev. B.01[2]. Geometry optimizations were performed using the M06-2X[3] functional with the Karlsruhe-family basis set of double-ζ valence def2-SVP[4,5] for all atoms. Minima and transition structures on the potential energy surface (PES) were confirmed using harmonic frequency analysis at the same level of theory, showing respectively zero and one imaginary frequency. Gibbs energies were evaluated at the reaction temperature of 30ºC, using a quasi-RRHO treatment of vibrational entropies[6], using the Good Vibes code[7]. Vibrational entropies of frequencies below 100 cm^{-1} were obtained according to a free rotor description, using a smooth damping function to interpolate between the two limiting descriptions. The free energies were further corrected using standard concentration of 1 mol/L, which were used in solvation calculations.

Single point (SP) corrections were performed using the domain-based local pair natural orbital – coupled cluster with perturbative triple excitations (DLPNO-CCSD(T)) calculations[8,9] using ORCA version 5.0.1[10-12]. T_0 approximation which neglects the couplings between different triples by the off-diagonal Fock matrix elements, instead of the recently published iterative T_1 algorithm[13], was employed. The NormalPNO settings with $T_{cutPairs} = 10^{-4}$, $T_{CutDO} = 10^{-2}$, $T_{CutPNO} = 3.33\times10^{-7}$ and $T_{CutMKN} = 10^{-3}$ was used throughout. The TightSCF convergence with KDIIS algorithm[14] for SCF iterations were used. The complete basis set (CBS) extrapolation scheme of Helgaker et al[15-17], was performed using either the correlation-consistent double-/triple-ζ cc-pV(DT)Z basis set[18-20] or the aug-cc-pV(DT)Z[21-22] basis sets, which are augmented with diffuse functions. The auxiliary basis sets required for the integral evaluations in the DLPNO-CCSD(T) correlation energy calculations were generated automatically using the "AutoAux" command from the automated auxiliary basis set construction module[23] of ORCA. DEFGRID2 grid for integration was employed throughout.

For the basis sets augmented with diffuse functions, the aug-cc-pV(DT)Z basis set produces linear dependency errors due to the addition of diffuse functions using the

"AutoAux" command, in this case, DLPNO-CCSD(T) was run separately with aug-cc-pVDZ or aug-cc-pVTZ basis set with corresponding auxiliary basis sets aug-cc-pVD(T)Z/C[21,24] and the obtained values are extrapolated manually according to the following formulae:

$$E_{\mathrm{SCF}}^{(X)} = E_{\mathrm{SCF}}^{(\infty)} + A\exp(-\alpha\sqrt{X}) \qquad \text{Eq (1)}$$

$$E_{corr}^{(\infty)} = \frac{X^{\beta}E_{\mathrm{corr}}^{(X)} - Y^{\beta}E_{\mathrm{corr}}^{(Y)}}{X^{\beta} - Y^{\beta}} \qquad \text{Eq (2)}$$

for the extrapolation of HF energy (Eq (1)) and of correlation energy (Eq (2)) to the basis set limit, respectively. $E_{\mathrm{SCF}/corr}^{(X)}$ is the SCF/correlation energy calculated with basis set of cardinal number *X*, and $E_{\mathrm{SCF}/corr}^{(\infty)}$ is the basis set limit SCF/correlation energy and *A, α,* and *β* are constants. For correlation energy, *X* and *Y* are the cardinal numbers of the basis sets used for extrapolation (*X*=2, *Y*=3 herein). For Extrapolate(2/3, cc), *α*=4.42*,* and *β*=2.46 and for Extrapolate(2/3, aug-cc), *α*=4.3*,* and *β*=2.51.

The integral equation formalism variant of the polarizable continuum model (IEF-PCM) with the SMD implicit continuum solvation model[25] was included to account for the solvent effect of toluene. Unless otherwise stated, the final SMD (toluene)-DLPNO-CCSD(T)/ cc-pV(DT)Z//M06-2X/def2-SVP Gibbs energies are used for discussion throughout. *All Gibbs energy values in the text and figures are quoted in kcal mol*$^{-1}$. All molecular structures and molecular orbitals were visualized using *PyMOL* software[26].

Geometries of all optimized structures (in *.xyz* format with their associated energy in Hartrees) are included in a separate folder named *optimised_xyz_structures* with an associated README file. All these data have been deposited and uploaded to zenodo.org (DOI: 10.5281/zenodo.5573970) under open access.

Model system calculation

To initially explore the potential energy surface of this reaction and to increase computational efficiency, we carried out a model calculation in which a model NHC and a model imine is used (Supplementary Figure 3). Note that for the model NHC used,

the reaction centre is similar as the chiral NHC catalyst used in the reaction. For the imine simplification, we note that the methanesulfinate group has similar reactivity as *p*-toluenesulfinate group. We use this model reaction to determine the key steps for the overall transformation, from which we applied the full model to the key step to determine the stereoselectivity.

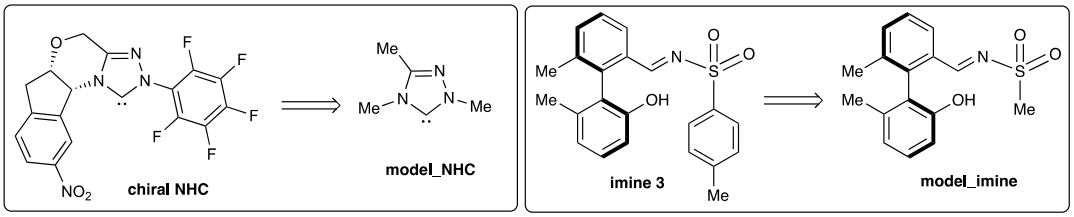

Supplementary Figure 3. Model NHC and model imine used for the calculation of Gibbs energy profile.

The full Gibbs energy profile for this model reaction is shown in Supplementary Figure 4. The Gibbs energies were calculated at SMD(Toluene)-DLPNO-CCSD(T)/ CBS//M06-2X/def2-SVP, using complete basis set (CBS) extrapolation at (2/3,cc) or (2/3,aug-cc) (in square brackets) procedure as outlined in the computational methods section. The reaction proceeds with firstly the addition of NHC catalyst to the imine C=N bond, giving a highly exergonic adduct **model_INT2**, at -9.3 [-8.5] kcal mol^{-1}. This is followed by the loss of methanesulfinate anion, via transition state, **model_TS2**, at 23.9 [23.7] kcal mol^{-1}. The final deprotonation of imine intermediate via **model_TS3**, regenerates the NHC catalyst and yields the nitrile product. We note that the use of basis set augmented with diffuse functions (aug-cc-pVD(T)Z) gives similar energies (within 1 kcal mol^{-1}) as the basis set not augmented with diffuse functions (cc-pVD(T)Z), thus, for full system calculations, we use Extrapolate(2/3,cc) without diffuse functions for increased computational efficiency.

We herein focus on the steps of NHC addition and the loss of methanesulfinate since these steps are likely stereo-determining in the overall transformation of the full system as the regeneration of NHC catalyst via **model_TS3** through deprotonation is likely facile and simply carries the stereochemical information from previous steps forward. From the Gibbs energy profile in Supplementary Figure 4, we can see that the

NHC adduct, **model_INT2**, is the resting state of the catalytic cycle. The rate-limiting step is the loss of methanesulfinate, **model_TS2**, with an energetic span of 33.2 [32.2] kcal mol^{-1} (from **model_INT2** to **model_TS2**). Moreover, the addition of NHC, **model_TS1**, is reversible, as the subsequent loss of methanesulfinate has a barrier of 33.2 [32.2] kcal mol^{-1}, which is higher than the barrier for the reversible process of adduct dissociation (going from **model_INT2** to **model_INT1**) with a barrier of 24.4 [24.4] kcal mol^{-1}. We note that this rate-limiting barrier is very high and is not consistent with the good reactivity at ambient temperature used for the reaction. We further carried out investigation of the full system to determine the energetic span for the actual system used in the reaction (*vide infra*).

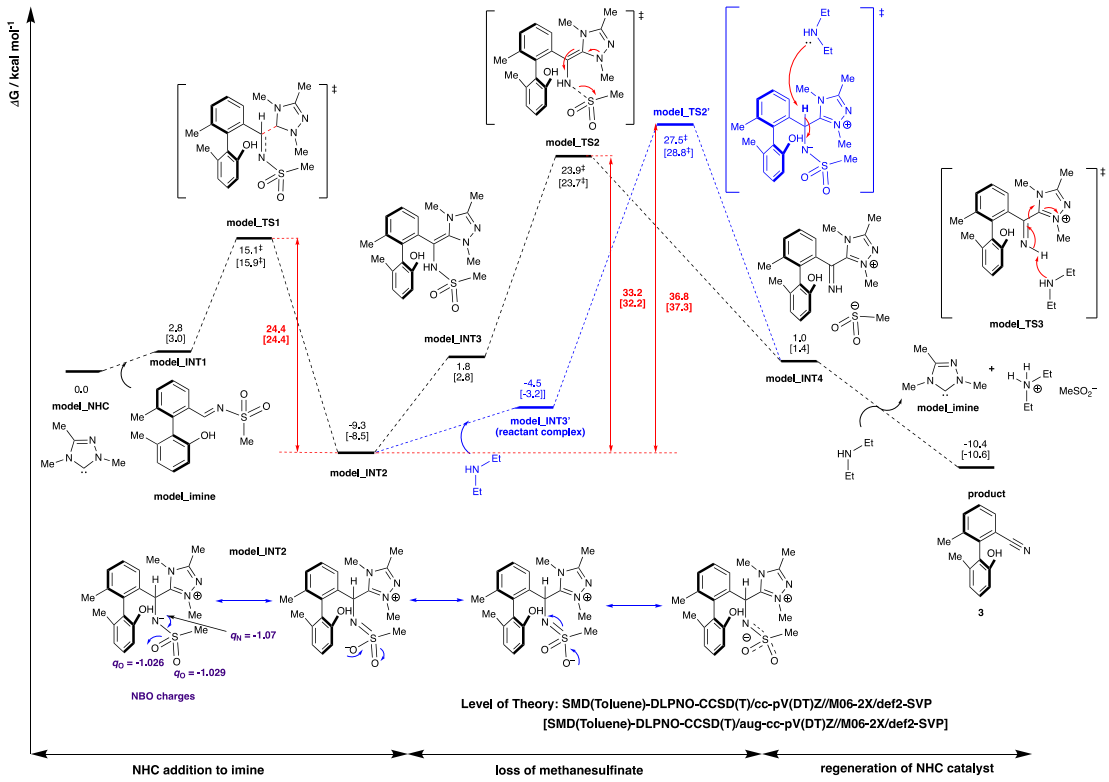

Supplementary Figure 5. Gibbs energy profile for the model reaction calculated at SMD(Toluene)-DLPNO-CCSD(T)/CBS//M06-2X/def2-SVP, using complete basis set (CBS) extrapolation at (2/3,cc) or (2/3,aug-cc) (in square brackets) procedure.

We also checked the alternative mechanism, in which the base-assisted deprotonation of the NHC-imine adduct via **model_TS2'** occurs to give the imine intermediate **model_INT4** directly, as proposed in a previous study of NHC-catalysed desulfonylation of tosylated aldimines[27]. However, this TS (**model_TS2'** at 27.5 [28.8]

kcal mol^{-1}) has an energetic span that is 3.6 [5.1] kcal mol^{-1} higher than the loss of methanesulfinate from the aza-Breslow intermediate (**model_TS2**). With these results, we focus on the step of loss of anion in the full system as both the rate-limiting and stereo-determining step.

Key steps and key transition state structures for the full reaction

major_TS2	**minor_TS2**
$\Delta G^{‡}$ = 23.7 kcal mol^{-1}	$\Delta G^{‡}$ = 27.2 kcal mol^{-1}
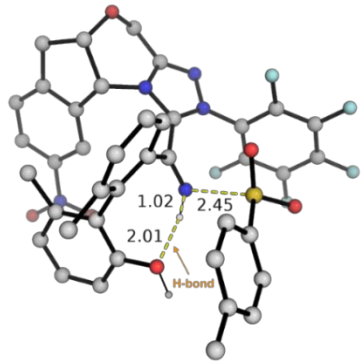	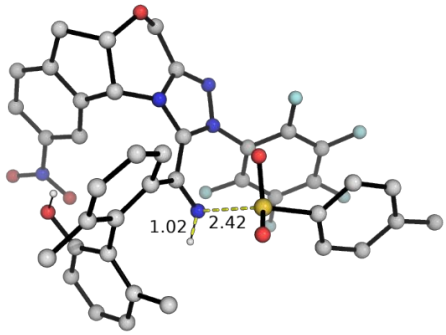
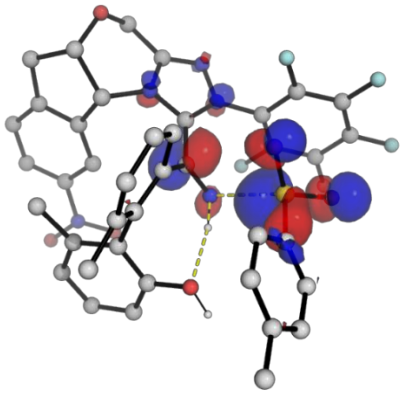	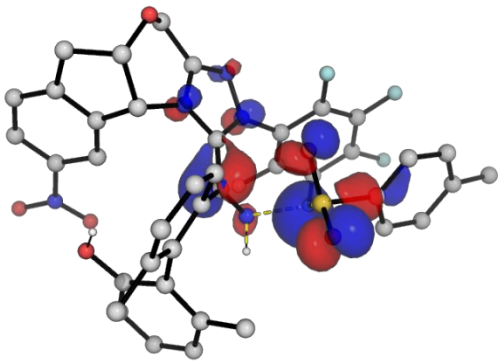

Supplementary Figure 6. DFT optimized transition state structures and their HOMO plots for the rate-determining step of loss of *p*-toluenesulfinate in the full reaction.

For the full reaction, we focus on the step of loss of toluenesulfinate from the Breslow intermediate as reflected by **model_TS2** in Supplementary Figure 5. Conformational sampling was carried out at the GFN2-xTB[28] level of theory using the *crest* program[29-31] from Grimme and co-workers. Note that since no TS structure could be located on the GFN2-xTB potential energy surface, we performed conformational

sampling on the aza-Breslow intermediate. A total of 104 conformers were located by the crest program, and these are sorted into 19 clusters of distinct conformers using the clustering_traj.py[32] with an RMSD cutoff of 1.0 Å (excluding H atoms). The 4 lowest energy structures were reoptimised at M06-2X/def2-SVP level of theory to yield the relevant TS structures for the rate- determining step of loss of toluenesulfinate. The lowest Gibbs energy structures for the TSs leading to both major and minor products, **major_TS2** and **minor_TS2**, respectively, are shown in Figure 6.

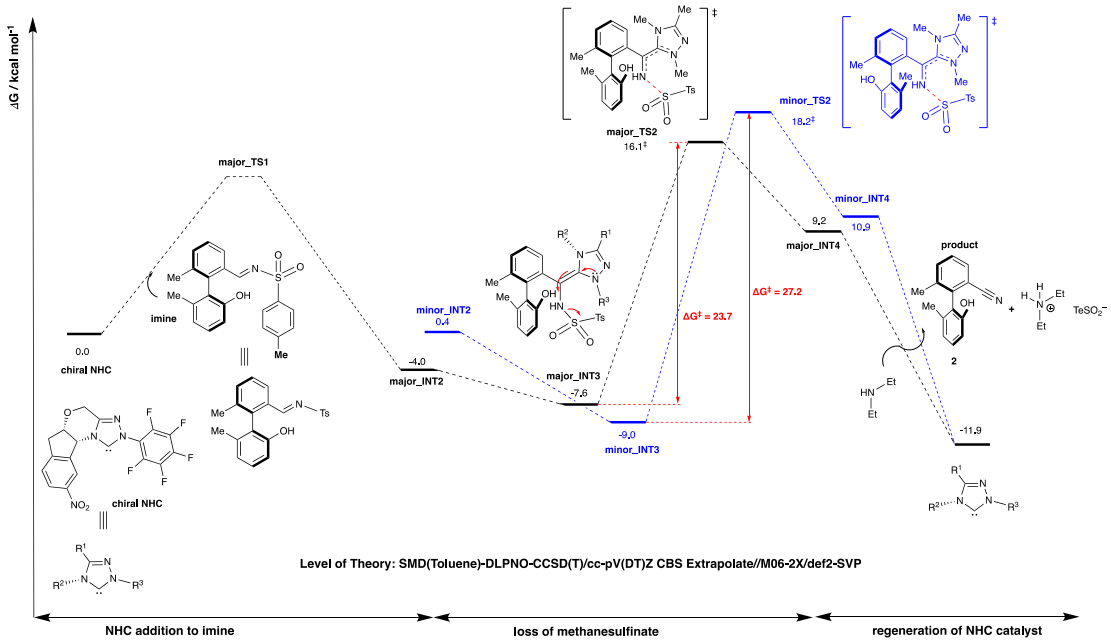

Supplementary Figure 6. Gibbs energy profile for the key steps of the full reaction calculated at SMD(Toluene)-DLPNO-CCSD(T)/cc-pV(DT)Z CBS Extrapolation//M06-2X/def2-SVP.

The Gibbs energy profile for the key step of the full system is shown in Supplementary Figure 6. The energetic span for the rate-determining TS leading to the major product is 23.7 kcal mol^{-1} and to the minor product is 27.2 kcal mol^{-1}. This barrier difference of 3.5 kcal mol^{-1} translates to an enantiomeric excess of 99%, at experimental temperature of 30°C, which is in good agreement with experimental observations. In addition, the energetic span of 23.7 kcal mol^{-1} is consistent with excellent reactivity at experimental temperature of 30°C. Their HOMO structures are

similar, and **major_TS2** is likely more favoured due to the hydrogen bonding formed between the OH group on the substrate and the amine group of the Breslow intermediate.

Rotational barriers for atropisomers

Supplementary Figure 7 shows the relaxed PES scan about the dihedral angles for the barriers of isomerisation of atropisomers of (a) **1a**, (b) **3a**, and (c) condensed imine. The barriers for isomerisation are all well over 50 kcal mol^{-1}, indicating that these atropisomers will not racemise easily at the reaction temperature of 30 ^{o}C.

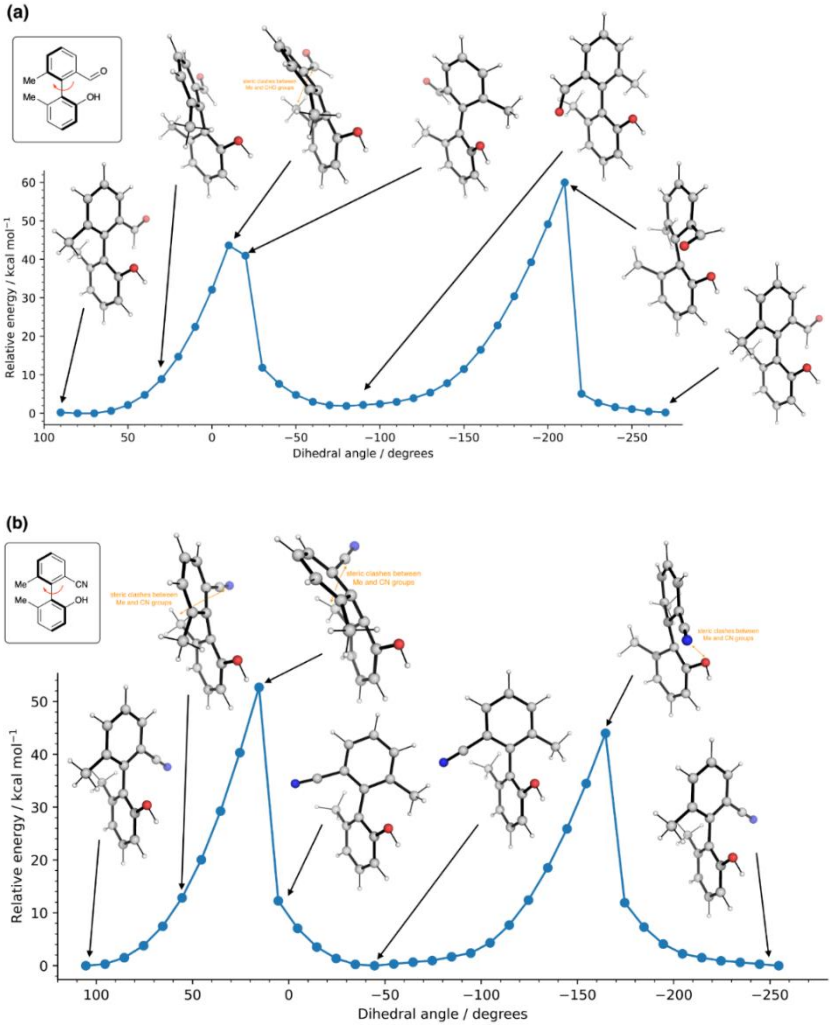

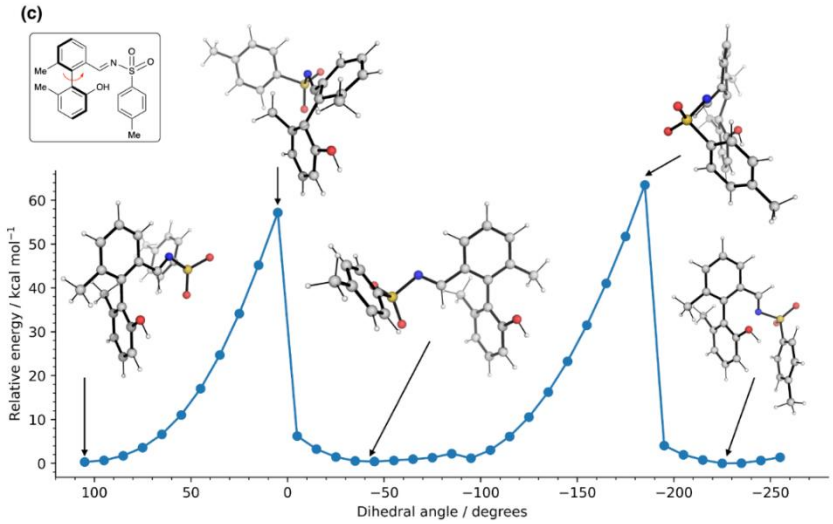

Supplementary Figure 7. Relaxed PES scan about the dihedral angles for the barriers of isomerisation of atropisomers of (a) substrate **1a**, (b) product **3a**, and (c) condensed imine

Optimised structures and absolute energies, zero-point energies

Geometries of all optimized structures (in *.xyz* format with their associated energy in Hartrees) have been deposited and uploaded to zenodo.org (DOI: 10.5281/zenodo. 5573970) under open access.

Absolute values (in Hartrees) for SCF energy, zero-point vibrational energy (ZPE), enthalpy and quasi-harmonic Gibbs free energy (at 30 ^{o}C/303.15 K) for optimised structures are given below. Single point corrections in SMD toluene using DLPNO-CCSD(T)/cc-pV(DT)Z CBS Extrapolate level of theory are also included (Supplementary Table 4). The individual energy values for (aug-)cc-pV(DT)Z basis sets and for extrapolated energies are included in Supplementary Table 5 and Supplementary Table 6.

Supplementary Table 4. Optimised structures and absolute energies, zero-point energies

Structure	E/au	ZPE/au	H/au	T.S/au	qh-G/au	SP SMD (toluene) DLPNO-CCSD(T) /cc-pV(DT)Z CBS Extrapolate
model_system						
Et_2NH_2Ms	-802.26423	0.209038	-802.04122	0.050974	-802.09067	-802.106771761
model_imine	-1297.3011	0.303744	-1296.9757	0.069216	-1297.0413	-1297.057584649
model_NHC	-359.72744	0.144296	-359.57359	0.039996	-359.61336	-359.734096841
model_INT1	-1657.0724	0.449095	-1656.592	0.089979	-1656.6768	-1656.808959381
model_TS1	-1657.0516	0.44998	-1656.5711	0.086668	-1656.6537	-1656.791717706
model_INT2	-1657.0875	0.452629	-1656.6046	0.086001	-1656.6865	-1656.833728768
model_INT3	-1657.0826	0.451871	-1656.6004	0.085618	-1656.682	-1656.815595236
model_TS2	-1657.0514	0.450388	-1656.5709	0.084953	-1656.6522	-1656.778899839
model_INT4	-1657.078	0.449421	-1656.5976	0.087806	-1656.681	-1656.813275761
model_INT3'	-1870.6262	0.604494	-1869.9829	0.106287	-1870.0821	-1870.382825950
model_TS2'	-1870.5768	0.600681	-1869.9385	0.101509	-1870.0344	-1870.330222484
Full system						
NHC	-1633.1919	0.262908	-1632.9043	0.07842	-1632.9774	-1633.365826
substrate_1	-729.63651	0.252446	-729.36729	0.056997	-729.4226	-729.5741718
substrate_1-c2	-729.63341	0.252251	-729.36439	0.0568	-729.41954	-729.5719554
$TsNH_2$	-874.78436	0.155925	-874.61621	0.048451	-874.66261	-874.5913381
Et_2N	-213.51354	0.150026	-213.35549	0.035622	-213.39093	-213.5363377
product	-708.58387	0.241686	-708.32566	0.056235	-708.38037	-708.4984566
major_TS2	-3161.3151	0.649318	-3160.6149	0.132663	-3160.737	-3161.1548
major_TS2-c2	-3161.3219	0.649753	-3160.6214	0.133526	-3160.7436	-3161.153644
major_TS2-c3	-3161.3099	0.649559	-3160.6099	0.132688	-3160.7315	-3161.15015
major_TS2-c4	-3161.3099	0.650099	-3160.609	0.134329	-3160.7313	-3161.144974
minor_TS2	-3161.3158	0.649746	-3160.6153	0.133319	-3160.7375	-3161.151609
major_INT2	-3161.3385	0.651677	-3160.6368	0.130192	-3160.756959	-3161.190316
major_INT3	-3161.3527	0.651003	-3160.6507	0.133176	-3160.772938	-3161.194197

major_INT4	-3161.3198	0.650182	-3160.618	0.135629	-3160.741952	-3161.165459
minor_INT2	-3161.3296	0.652316	-3160.6271	0.132009	-3160.748028	-3161.183229
minor_INT3	-3161.3596	0.651797	-3160.6571	0.132231	-3160.77859	-3161.197593
minor_INT4	-3161.3377	0.651058	-3160.6356	0.133459	-3160.758143	-3161.169332

Supplementary Table 5. Raw energy values obtained at SMD(toluene)-DLPNO-CCSD(T)/cc-pV(DT)Z basis sets and the complete basis set (CBS) extrapolation. Final single-point (SP) energy = Extrapolated SCF energy + Extrapolated correlation energy. $\alpha = 4.42$ and $\beta = 2.46$ in the extrapolation of SCF and correlation energies. All values have the units of a.u.

Structure	**SCF with SMD correction**			**Correlation**			**Final SP Energy**
	cc-pVDZ	**cc-pVTZ**	**Extrapolated**	**cc-pVDZ**	**cc-pVTZ**	**Extrapolated**	
model_system							
Et_2NH_2Ms	-799.739799018	-799.905382516	-799.959232958	-1.567095981	-1.933459369	-2.147538803	-802.106771761
model_imine	-1292.350713901	-1292.651932034	-1292.749893061	-3.196967918	-3.898033504	-4.307691588	-1297.057584649
model_NHC	-357.922994234	-358.016208822	-358.046523720	-1.268622429	-1.533055357	-1.687573121	-359.734096841
model_INT1	-1650.270396404	-1650.656738374	-1650.782383055	-4.490820235	-5.460157409	-6.026576326	-1656.808959381
model_TS1	-1650.239943402	-1650.627614341	-1650.753691224	-4.499830286	-5.470707603	-6.038026482	-1656.791717706
model_INT2	-1650.267354080	-1650.656000373	-1650.782394457	-4.505104472	-5.481052457	-6.051334311	-1656.833728768
model_INT3	-1650.244898291	-1650.633466029	-1650.759834565	-4.511204910	-5.486096252	-6.055760671	-1656.815595236
model_TS2	-1650.205846635	-1650.580614833	-1650.702495535	-4.530162627	-5.506118084	-6.076404304	-1656.778899839
model_INT4	-1650.268556189	-1650.636595358	-1650.756287670	-4.511122175	-5.486840459	-6.056988091	-1656.813275761
model_INT3'	-1862.599799293	-1863.042477792	-1863.186444026	-5.373794166	-6.524173499	-7.196381924	-1870.382825950
model_TS2'	-1862.5208	-1862.9616	-1863.1049	-5.3995017	-6.5518600	-7.2252248	-1870.33022

	92530	54638	97631	67	53	54	2484
Full System							
NHC	-1626.335619693	-1626.792485702	-1626.941065945	-4.653597280	-5.771518237	-6.424760054	-1633.365826
substrate_1	-725.980592246	-726.162570798	-726.221753178	-2.520900897	-3.045737493	-3.352418578	-729.5741718
substrate_1-c2	-725.975835382	-726.158165793	-726.217462602	-2.522014761	-3.047457520	-3.354492809	-729.5719554
$TsNH_2$	-871.981523630	-872.180990155	-872.245859907	-1.715663631	-2.113189408	-2.345478158	-874.5913381
Et_2N	-212.337812151	-212.398958746	-212.418844611	-0.845185687	-1.017060424	-1.117493075	-213.5363377
product	-704.983965067	-705.157047882	-705.213337223	-2.481844577	-2.988854842	-3.285119355	-708.4984566
major_TS2	-3148.174727490	-3148.960491447	-3149.216034643	-8.774931548	-10.771877556	-11.938765637	-3161.1548
major_TS2-c2	-3148.189755503	-3148.972161576	-3149.226612733	-8.765892068	-10.761137393	-11.927031704	-3161.153644
major_TS2-c3	-3148.180046923	-3148.965769449	-3149.221299171	-8.767520697	-10.762886435	-11.928851106	-3161.15015
major_TS2-c4	-3148.168054423	-3148.951663987	-3149.206506538	-8.775440768	-10.771877222	-11.938467552	-3161.144974
minor_TS2	-3148.209500774	-3148.990916285	-3149.245045294	-8.755708696	-10.751434603	-11.917609735	-3161.151609
major_INT2	-3148.204604326	-3149.001066214	-3149.260088550	-8.768032799	-10.763943939	-11.930227310	-3161.190316
major_INT3	-3148.214708086	-3149.013755581	-3149.273618799	-8.757724218	-10.754051614	-11.920578217	-3161.194197
major_INT4	-3148.206734153	-3148.989408987	-3149.243947549	-8.758592967	-10.754960817	-11.921511059	-3161.165459
minor_INT2	-3148.203946802	-3149.001562434	-3149.260959986	-8.759615265	-10.755816345	-11.922269138	-3161.183229
minor_INT3	-3148.224743854	-3149.022932938	-3149.282516986	-8.753887927	-10.749163877	-11.915076083	-3161.197593
minor_INT4	-3148.225126187	-3149.002381899	-3149.255158075	-8.751976839	-10.747889320	-11.914173473	-3161.169332

Supplementary Table 6. Raw energy values obtained at SMD(toluene)-DLPNO-CCSD(T)/aug-cc-pV(DT)Z basis sets and the complete basis set (CBS) extrapolation. Final single-point (SP) energy = Extrapolated SCF energy + Extrapolated correlation energy. $\alpha = 4.3$ and $\beta = 2.51$ in the extrapolation of SCF and correlation energies. All values have the units of a.u.

Structure	SCF with SMD correction			Correlation			Final SP Energy
	aug-cc-pVDZ	aug-cc-pVTZ	Extrapolated	aug-cc-pVDZ	aug-cc-pVTZ	Extrapolated	
model_system							
Et_2NH_2Ms	-799.7758716	-799.9109926	-799.9572291	-1.659181162	-1.971594274	-2.148411339	-802.1056405
model_imine	-1292.408135117	-1292.662054645	-1292.74894238804	-3.353900919	-3.965305314	-4.311343064947602	-1297.060285
model_NHC	-357.939275380	-358.019936405	-358.047537489756	-1.323241590	-1.557165410	-1.689559735634299 3	-359.7370972
model_INT1	-1650.338229680	-1650.668620860	-1650.781676142 42	-4.712067730	-5.555390570	-6.032687660539143	-1656.814364
model_TS1	-1650.310912401	-1650.640011619	-1650.752624809 93	-4.727326343	-5.567849786	-6.043562496299464	-1656.796187
model_INT2	-1650.341098744	-1650.668968362	-1650.781160800 85	-4.737187838	-5.579968453	-6.056958659386785	-1656.838119
model_INT3	-1650.315461981	-1650.645849460	-1650.758903475 99	-4.740759689	-5.583729768	-6.060827205700431 5	-1656.819731
model_TS2	-1650.280608887	-1650.594754261	-1650.702250453 78	-4.763910398	-5.606086280	-6.082734224458418	-1656.784985
model_INT4	-1650.339200377	-1650.649982339	-1650.756327618 81	-4.744216551	-5.585749661	-6.062033814522222	-1656.818361
model_INT3'	-1862.679457	-1863.055777	-1863.184548	-5.651295149	-6.642073905	-7.202826911	-1870.387375
model_TS2'	-1862.601845	-1862.975486	-1863.103341	-5.680425641	-6.670776173	-7.231286816275702	-1870.334628
diethylamine	-212.3490230 14	-212.4013444 25	-212.4192480 86645	-0.880787770	-1.032243922	-1.117963858 9743786	-213.5372119
product	-705.009968746	-705.163111799	-705.215515229103	-2.583703204	-3.033408046	-3.287928382 1122827	-708.5034436

References:

Full reference for Gaussian software:

Gaussian 16, Revision A.01, Frisch, M. J.; Trucks, G. W.; Schlegel, H. B.; Scuseria, G. E.; Robb, M. A.; Cheeseman, J. R.; Scalmani, G.; Barone, V.; Mennucci, B.; Petersson, G. A.; Nakatsuji, H.; Caricato, M.; Li, X.; Hratchian, H. P.; Izmaylov, A. F.; Bloino, J.; Zheng, G.; Sonnenberg, J. L.; Hada, M.; Ehara, M.; Toyota, K.; Fukuda, R.; Hasegawa, J.; Ishida, M.; Nakajima, T.; Honda, Y.; Kitao, O.; Nakai, H.; Vreven, T.; Montgomery Jr., J. A.; Peralta, J. E.; Ogliaro, F.; Bearpark, M.; Heyd, J. J.; Brothers, E.; Kudin, K. N.; Staroverov, V. N.; Kobayashi, R.; Normand, J.; Raghavachari, K.; Rendell, A.; Burant, J. C.; Iyengar, S. S.; Tomasi, J.; Cossi, M.; Rega, N.; Millam, J. M.; Klene, M.; Knox, J. E.; Cross, J. B.; Bakken, V.; Adamo, C.; Jaramillo, J.; Gomperts, R.; Stratmann, R. E.; Yazyev, O.; Austin, A. J.; Cammi, R.; Pomelli, C.; Ochterski, J. W.; Martin, R. L.; Morokuma, K.; Zakrzewski, V. G.; Voth, G. A.; Salvador, P.; Dannenberg, J. J.; Dapprich, S.; Daniels, A. D.; Farkas, Ö.; Foresman, J. B.; Ortiz, J. V; Cioslowski, J.; Fox, D. J. Gaussian, Inc., Wallingford CT, 2016.

1. Guo, D., Zhang, J., Zhang, B. & Wang, J. Ruthenium-catalyzed atropoenantioselective synthesis of axial biaryls via reductive amination and dynamic kinetic resolution. *Org. Lett*. **20**, 6284-6288 (2018).

2. Frisch, M. J. et al. Gaussian 16, Revision B.01. 2016.

3. Zhao, Y. & Truhlar, D. G. The M06 suite of density functionals for main group thermochemistry, thermochemical kinetics, noncovalent interactions, excited states, and transition elements: Two new functionals and systematic testing of four Mo6-class functionals and 12 other function. *Theor. Chem. Acc.* **120**, 215–241 (2008).

4. Weigend, F. & Ahlrichs, R. Balanced basis sets of split valence, triple zeta valence and quadruple zeta valence quality for H to Rn: Design and assessment of accuracy. *Phys. Chem. Chem. Phys.* **7**, 3297–3305 (2005).

5. Weigend, F. Accurate coulomb-fitting basis sets for H to Rn. *Phys. Chem. Chem. Phys.* **8**, 1057–1065 (2006).

6. Grimme, S. Supramolecular binding thermodynamics by dispersion-corrected density functional theory. *Chem. Eur. J.* **18**, 9955–9964 (2012).

7. Luchini, G., Alegre-Requena, J. V., Funes-Ardoiz, I. & Paton, R. S. GoodVibes: Automated thermochemistry for heterogeneous computational chemistry data. *F1000Research*, **9**, 291 (2020).

8. Riplinger, C. & Neese, F. An efficient and near linear scaling pair natural orbital based local coupled cluster method. *J. Chem. Phys.* **138**, 034106 (2013).

9. Riplinger, C., Sandhoefer, B., Hansen, A. & Neese, F. Natural triple excitations in local coupled cluster calculations with pair natural orbitals. *J. Chem. Phys.* **139**, 134101 (2013).

10. Neese, F. The ORCA program system. *Wiley Interdiscip. Rev. Comput. Mol. Sci.* **2**, 73–78 (2012).

11. Neese, F. Software Update: The ORCA program system, Version 4.0. *Wiley Interdiscip. Rev. Comput. Mol. Sci.* **8**, e1327 (2018).

12. Neese, F., Wennmohs, F., Becker, U. & Riplinger, C. The ORCA quantum chemistry program package. *J. Chem. Phys.* **152**, 224108 (2020).

13. Guo, Y.; Riplinger, C.; Becker, U.; Liakos, D. G.; Minenkov, Y.; Cavallo, L.; Neese, F. An Improved Linear Scaling Perturbative Triples Correction for the Domain Based Local Pair-Natural Orbital Based Singles and Doubles Coupled Cluster Method [DLPNO- CCSD(T)]. *J. Chem. Phys.* **148**, 011101 (2018).

14. Kollmar, C. The role of energy denominators in self-consistent field (SCF) calculations for open shell systems", *J. Chem. Phys.* 105, 8204. (1996)

15. Halkier, A. et al. Basis-set convergence in correlated calculations on Ne, N_2 , and H_2O. *Chem. Phys. Lett.* **286**, 243–252 (1998).

16. Helgaker, T., Klopper, W., Koch, H. & Noga, J. Basis-set convergence of correlated calculations on Water. *J. Chem. Phys.* **106**, 9639–9646 (1997).

17. Halkier, A., Helgaker, T., Jørgensen, P., Klopper, W. & Olsen, J. Basis-set convergence of the energy in molecular hartree-fock calculations. *Chem. Phys. Lett.* **302**, 437–446 (1999).

18. Dunning, T. H. Gaussian basis sets for use in correlated molecular calculations. I. The atoms boron through neon and hydrogen. *J. Chem. Phys.* **90**, 1007–1023 (1989).

19. Woon, D. E. & Dunning, T. H. Gaussian basis sets for use in correlated molecular calculations. III. The atoms aluminum through argon. *J. Chem. Phys.* **98**, 1358–1371 (1993).

20. Woon, D. E. & Dunning, T. H. Gaussian basis sets for use in correlated molecular calculations. V. Core-valence basis sets for boron through neon. *J. Chem. Phys.* **103**, 4572–4585 (1995).

21. Kendall, R. A.; Dunning, Jr., T. H.; Harrison, R. J. Electron affinities of the first-row atoms revisited. Systematic basis sets and wave functions. *J. Chem. Phys.* **96**, 6796 (1992)

22. Woon, D. E. & Dunning, T. H. *J.* Gaussian basis sets for use in correlated molecular calculations. III. The atoms aluminum through argon. *Chem. Phys.* **98**, 1358 (1993).

23. Stoychev, G. L.; Auer, A. A.; Neese, F. Automatic Generation of Auxiliary Basis Sets. *J. Chem. Theory Comput.* **13**, 554, (2017).

24. Provasi, P. F.; Aucar, G. A.; Sauer, S. P. A. The effect of lone pairs and electronegativity on the indirect nuclear spin–spin coupling constants in CH2XCH2X (X=CH2,(X=CH2, NH, O, S): *Ab initio* calculations using optimized contracted basis sets. *J. Chem. Phys.* **115**, 1324 (2001).

25. Marenich, A. V., Cramer, C. J. & Truhlar, D. G. Universal solvation model based on solute electron density and on a continuum model of the solvent defined by the bulk dielectric constant and atomic surface tensions. *J. Phys. Chem. B* **113**, 6378–6396 (2009).

26. Schrödinger, L. The PyMOL molecular graphics development component*, Version 1*. **8**, (2015).

27. Sun, F. et al. A Combined experimental and computational study of NHC-promoted desulfonylation of tosylated aldimines. *Org. Chem. Front.* **7**, 578–583 (2020).

28. Bannwarth, C., Ehlert, S. & Grimme, S. GFN2-xTB - An accurate and broadly parametrized self-consistent tight-binding quantum chemical method with multipole

electrostatics and density-dependent dispersion contributions. *J. Chem. Theory Comput.* **15**, 1652–1671 (2019).

29. Pracht, P. & Grimme, S. Calculation of absolute molecular entropies and heat capacities made simple. *Chem. Sci.* **12**, 6551–6568 (2021).

30. Grimme, S. Exploration of chemical compound, conformer, and reaction space with meta-dynamics simulations based on tight-binding quantum chemical calculations. *J. Chem. Theory Comput.* **15**, 2847–2862 (2019).

31. Pracht, P., Bohle, F. & Grimme, S. Automated exploration of the low-energy chemical space with fast quantum chemical methods. *Phys. Chem. Chem. Phys.* **22**, 7169–7192 (2020).

32. Cezar, H. M. Clustering traj https://github.com/hmcezar/clustering-traj. Accessed 07 Aug 2021.